Journal of the European Ceramic Society 20 (2000) 889–893

Alumina disks with different surface finish: thermal shock behavior

A.G. Tomba*, A.L. Cavalieri

Instituto de Investigaciones en Ciencia y Tecnología de Materiales, INTEMA, Av. J. B. Justo 4302, (7600) Mar del Plata, Argentina

Received 14 May 1999; accepted 16 August 1999

Abstract

Disks of commercial alumina powder were fabricated by slip casting and sintering (1600°C, 2 h). Two different surface treatments were performed: a coarse wear, using a 70 grit diamond wheel (CAW) and a fine one with SiC paper of 120 and 320 grit (FAW). The thermal shock resistance of the worn specimens was evaluated testing the disks by sudden cooling with a high-velocity air jet. The critical temperature differential (ΔT_C) was determined increasing the initial temperature of the sample in 10°C until the crack propagation was detected. The values of the mean ΔT_C were 940°C for FAW specimens and 765°C for CAW ones. The statistical distributions of the results were analyzed in function of the fracture strength of the specimens measured in biaxial flexion and the characteristics of the different surface finish determined by scanning electron microscopy, profilometry, and residual stresses measured by X-ray diffraction. © 2000 Elsevier Science Ltd. All rights reserved.

Keywords: Al_2O_3; Finishing; Surfaces; Thermal shock resistance

1. Introduction

In spite of the several advantages of ceramics — chemical inertia, refractoriness and excellent mechanical properties at high temperatures — these materials are rather susceptible to damage or fracture under thermal shock conditions produced in service. Unfortunately, the great complexity of the material degradation under these conditions translates to the study of the thermal shock behavior. For instance, the lack of a unique and simple test restrains the obtainment of extrapolable data since they result closely linked to the experimental conditions and their analysis can not be done abstracting the experimental aspects.

The quenching in water is the most common method employed in traditional searching of thermal shock of ceramics.[1–6] The main drawbacks of this investigations are the difficulty in the extrapolation of the results to real service conditions and the typical limitations of the test:[7–11] a heat transfer coefficient too high with respect to that in service conditions and strongly dependent on the bath temperature are among the mayor disadvantage. Attempting to surmount these problems, recent studies are based on the calculation of the stresses arising during the thermal shock by the application of more realistic models that simulate the actual thermomechanical conditions with the minor simplifications. Novel techniques have been designed to satisfy the requirements of these approaches.[7,11–20]

In thermal shock by cooling, the surface of the body suffers the maximum stresses in tension. So, the behavior of the material subjected to this thermomechanical loading results strongly dependent on the surface features. The objective of the present work is to study the effects of different machining procedures on the thermal shock resistance of alumina ceramic materials, using a controlled cooling test.

2. Experimental procedure

2.1. Preparation of the specimens

A commercial high purity alumina powder (Reynolds RC-HP DBM, 0.35 μm, 7.3 m^2/g) was used as the raw material. Disks (radius: 35.00 ± 0.02 mm, height: 2.67 ± 0.01 mm) were fabricated by slip casting of an aqueous suspension of the powder. The green samples were calcined at 900°C, 1 h and pre-ground with SiC papers (120, 320 and 600 grit) before sintering at 1600°C, 2 h. Fired density, measured by Archimedes method in water, was 3.96 g/cm^3 (99.5% of the theoretical density).

* Corresponding author. Tel.: 54-223-481-6600; fax: +54-223-481-0046.

E-mail address: agtomba@fi.mdp.edu.ar (A.G. Tomba).

PII: S0955-2219(99)00232-0

The microstructure of the sintered material was homogeneous, with equiaxial and elongated grains (aspect ratio 2.6) and few intragranular pores. The mean grain size was 3.46 μm.

Two different surface treatments of the sintered disks were performed: coarse abrasive wear (CAW) and fine abrasive wear (FAW). The CAW operation was carried out using a resin-bonded 70 grit diamond wheel with a feed rate of 300 mm/min, an infeed of 0.05 mm and a wheel speed of 3800 rpm. The fine surface finishing (FAW) was achieved manually, using a semi-automatic polishing machine with a plate speed of 125 rpm and SiC paper of 120 and 320 grit, consecutively. Kerosene and water were employed as coolant/lubricant in CAW and FAW procedure, respectively.

2.2. Characterization

The worn surfaces were analyzed in a previous work[21] by scanning electron microscopy and surface roughness and residual stresses measurements. The fracture strength of the disks was determined in biaxial flexure. The main statements are given below.

The S.E.M. images are shown in Fig. 1. The CAW surface [Fig. 1(a)] showed a pronounced machining grooves with a well defined orientation while the action of the abrasive grains in the fine wear did not leave a directional pattern on the surfaces [Fig. 1(b)]. Both treated surfaces exhibited a lot of cavities together with smooth zones, the FAW surfaces having a more homogeneous microstructure than the CAW surfaces. A distinct relative contribution of the mechanisms of fragile fracture and plastic deformation was observed, the last being higher in CAW surfaces than in FAW ones.

Surface roughness of both specimens was measured. These measurements were done on CAW surfaces perpendicularly (⊥) and parallel (||) to the groove directions. The average roughness, *Ra*, as a measure of the superficial irregularities or texture, resulted slightly higher for the CAW surface ($0.719_{\perp}$, $0.659_{\|}$) than for the FAW surface (0.507). This is according to the fact that CAW surfaces are not completely smooth, even in the plastically deformed areas [Fig. 1(a)]. Additionally, the roughness in a parallel direction to the machining grooves was lower than that measured in a perpendicular one in CAW surfaces, as was expected. The same behavior was observed for the other roughness parameters *Rp* (maximum peak height) and *Rt* (maximum peak to valley height).

The measured residual stresses were in compression for both CAW and FAW specimens, with higher values for the first ones. The values obtained for the diffraction planes {1 0 10} and {1 1 9} were -147.94 ± 11.56 and -89.75 ± 4.73 MPa for the CAW surface and -91.28 ± 10.24 and -60.9 ± 7.21 MPa for the FAW one, respectively.

The fracture strength of both kinds of specimens was measured in biaxial flexure employing a ball on discontinuous ring fixture. The fracture strength obtained was higher for CAW specimens, 296 ± 59 MPa, than for FAW specimens, 220 ± 66 MPa. The same order was observed in the Weibull modulus: 11.0 for CAW and 6.9 for FAW.

The operative conditions of CAW finishing that introduced the more extended plastically deformed zones originating the higher compressive residual stresses and surface roughness, produced the higher values of biaxial flexion strengths with the lower dispersion of the data.

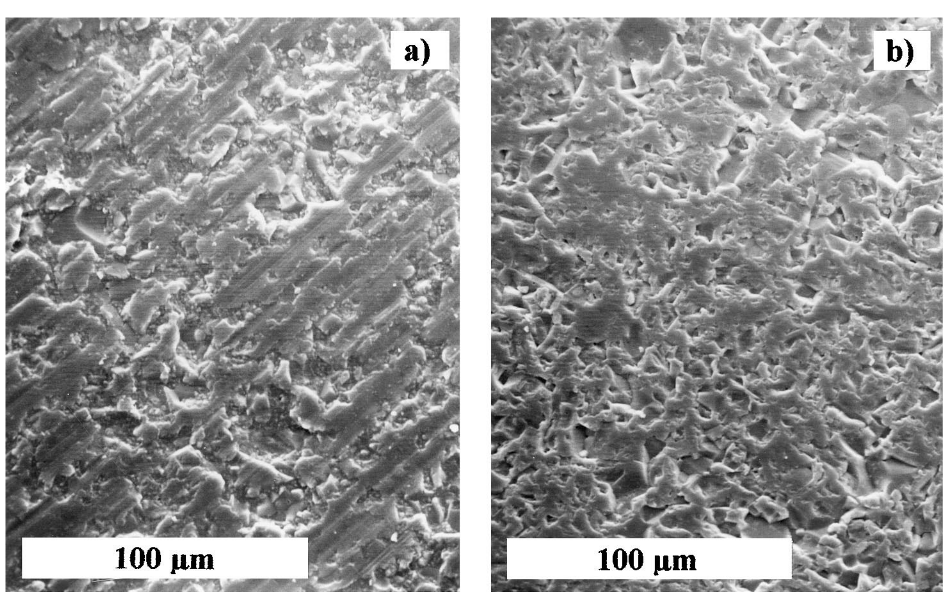

Fig. 1. S.E.M. micrographs of treated alumina surfaces: (a) CAW; (b) FAW.

2.3. Thermal shock tests

The specimens mounted horizontally on a refractory material were individually tested in thermal shock conditions using the apparatus shown in Fig. 2.[11,21] The upper surface was the machined one. The specimen was heated in an electrical furnace up to a predetermined temperature (T_i), allowed to equilibrate during 90 min and then subjected to a sudden temperature change using a high-velocity air jet (330 m/min) at room temperature (T_0 = 26–27°C). The air was channeled onto the disk center during 20 s, using a silica tube (3.58 ± 0.02 mm in inner diameter) placed at 90° and 3 mm above the tested surface. During the air impinging, the temperature of the sample was recorded on the central point of its lower surface, attaching a fast response Pt–10%Rh/Pt thermocouple.

After quenching, the specimens were cooled up to room temperature and examined for crack extension. If no cracking occurs, the temperature differential between the disk and the air jet ($\Delta T = T_i - T_0$) was incremented in 10°C until crack propagation was detected. Using this method, the thermal shock resistance T_C (or $\Delta T_C = T_C - T_0$) defined as the value of T_i which produces cracks (crack initiation condition), is evaluated. This value exhibits the dispersion typical of the ceramic material properties that depend on the flaw population. So, the data are reported as distributions of ΔT_C using a failure probability estimator (P_F) adequate to the sample size: $P_F = (i - 0.5)/N$ (i is the rank and N is the number of tested specimens).

The ranges of T_i that depend on the tested material resulted 770–940°C and 870–980°C for CAW and FAW specimens, respectively.

2.4. Thermal shock resistance parameter

Since the thermal shock test used gives information about the condition of damage initiation, the thermal shock resistance parameter suitable to evaluate the material behavior is R', defined by Eq. (1):

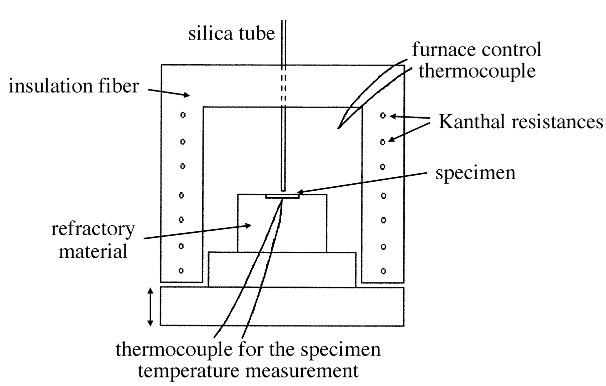

Fig. 2. Scheme of the thermal shock test apparatus.

$$R' = \frac{k\sigma_F(1-\nu)}{E\alpha} = kR \tag{1}$$

where k is the thermal conductivity, σ_F is the fracture strength, ν is the Poisson modulus, E is the Young modulus and α is the thermal expansion coefficient.

This parameter was calculated at 900°C, an intermediate temperature in the range of the tested T_i. The values of the alumina properties were taken from the literature at 900°C:[22] E = 381700 MPa, k = 6.3 W/m°C, ν = 0.26 and $\alpha = 8.14 \times 10^{-6}$°C^{-1}. The influence of the surface finish was introduced through the experimental mean fracture strength σ_F measured at room temperature (CAW: 296 MPa, FAW: 220 MPa).

3. Results and discussion

The ΔT_C distributions obtained for both surface finishes are plotted in Fig. 3. The statistical and thermal shock parameters are shown in Table 1.

A strong dependence of the temperature differential for cracking on the surface characteristics of the disks originated in the different finishing was determined. The probability curve for FAW specimens shifts to higher values of ΔT_C. However, the thermal shock resistance evaluated through the parameter R' is larger for CAW disks than for FAW ones. In turn, FAW specimens

Table 1
Statistical and thermal shock parameters for CAW and FAW alumina disks

	FAW	CAW
ΔT_C (°C)	916 ± 80	765 ± 90
Sd (°C)	54.25	51.60
R' (W/m)	330	444

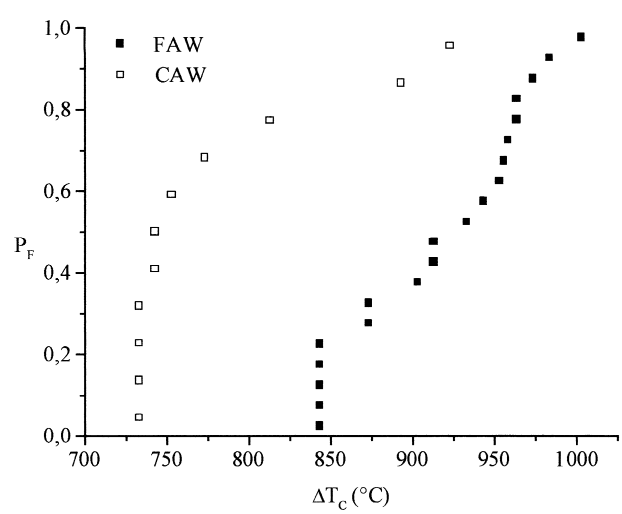

Fig. 3. Critical temperature differential distribution for CAW and FAW alumina specimens.

exhibit a slightly higher dispersion (*Sd*) than the CAW specimens. It is considered that the minimum value of ΔT_C has been slightly overevaluated since the existence of specimens broken at these T_i generates doubts about the possibility of cracking at lower values of T_i.

Since the thermal shock system employed produces the maximum tension in the central region of the tested surface,[11,13,21] the machined one, an influence of the surface features is expected, as much as it occurs in mechanical testing.

On one hand, the thermal shock tests as the used here allow the evaluation of the resistance to the fracture initiation by the thermal stresses through the value of ΔT_C. Also, on the basis of the thermoelasticity theory, the higher the ΔT, the higher the thermal stresses produced in the specimen subjected to thermal shock.[23,24] As a consequence, the specimen with the highest thermal shock resistance should have the largest ΔT_C, being able to support the highest thermal tension.

On the other hand, in general it is assumed that exists a parity between the behavior of the material under both, thermal and mechanical stresses.[11,13,15,18] It is opportune to point out here that the thermal shock and the biaxial flexure tests employed in this work were selected in order to produce an equivalent distribution of equibiaxial stresses in the central region of the specimen,[21] so, giving a greater support to the hypothesis of parity. On this basis, the material with the highest mechanical strength would exhibit the highest ΔT_C and also, the highest thermal shock resistance parameter R' since it is derived from the same assumption.

However, the experimental results do not follow this tendency: the FAW disks with the highest ΔT_C exhibit the lower mechanical strength and R' parameter. Which are the possible reasons to the disagreement between the experimental data and that expected based on the parity hypothesis? Let us attempt to analyze them.

First at all, the fact that the specimens were mechanically tested not at the thermal shock temperature range but at room temperature was considered no significative since the alumina suffers a slight variation of the mechanical properties up to 1100°C.[25] Moreover, the compressive residual stresses which may be responsible for the higher fracture strength of CAW specimens[21] should have the same effect on ΔT_C. However, since the relative ΔT_C values were not those expected on this basis, it is not discarded an annealing effect that relieves the residual stresses. The possible occurrence of this fact is associated to the methodology used here, in which the specimen is subjected to several exposure at high temperatures during a long period each time (90 min). This stress relaxation would modify the mechanical response of CAW as much as FAW disks and, in the extreme case, it could invert the order of σ_F, giving a possible reason to the relative magnitudes of ΔT_C values obtained.

At this point, it is worthwhile to note that a complete analysis of the material behavior under thermal shock conditions should include not only the thermal stresses related to the macroscopic ΔT, but also, the study of the actual heat transfer conditions between the specimen and the medium. These conditions determine, together with the thermomechanical properties of the material, the microscopic temperature distribution and, in turn, the stresses distribution. Specifically in this case, for instance, the dissimilar surface roughness in CAW and FAW disks influences the heat transfer by convection which will result in different values of the heat transfer coefficient (*h*): 320 $W/m^{2\circ}C$ for CAW and 230 $W/m^{2\circ}C$ for FAW.[21] As a consequence, the temperature and stress distributions depend on the surface finish,[21] and this could be other factor that contributes to explain the response of both materials.

It is important to emphasize that the obtained results are another evidence to the deficiency to use only the thermal shock parameters in the prediction or explanation of the ceramics behavior under sudden changes of temperature. This is understood having in mind that these figures of merit do not contemplate factors such as residual stresses and other microstructural features, which strongly condition the response of ceramics to thermal shock.

4. Conclusions

The thermal shock resistance evaluated through ΔT_C was strongly dependent on the resulting features of the disk surfaces due to the finishing. The specimens with the coarse wear producing the more extended plastically deformed areas associated with the higher compressive residual stress, surface roughness and biaxial flexion strength exhibited the lower resistance to the fracture initiation under thermal shock condition.

The relative magnitudes of ΔT_C for FAW and CAW specimens were inverse to those predicted on the basis of their mechanical strength values together with the parity hypothesis. A possible explanation was given through the relief of the residual stresses by annealing in the thermal shock conditions and the actual heat transfer coefficients determining the microscopic thermal stresses distributions.

The above facts have also been applied to account for the disagreement between the calculated thermal shock resistance parameter and the experimental results. It is evident that this parameter is not sufficient to predict the thermal shock behavior of ceramics by itself.

References

1. Singh, J. P., Thomas, J. R. and Hasselman, D. P. H., Analysis of effect of heat-transfer variables on thermal stress resistance of brittle ceramics measured by quenching experiments. *J. Am. Ceram. Soc.*, 1980, **63**, 140–144.

2. Lewis III, D., Thermal shock and thermal shock fatigue testing of ceramics with the water quench test. In *Fracture Mechanics of Ceramics*, Vol. 5, ed. R. Bradt, A. G. Evans, D. P. H. Hasselman and F. F. Lange. Plenum Press, New York, 1983, pp. 487–496.
3. Rogers, W. P., Emery, A. F., Bradt, R. C. and Kobayashi, A. S., Statistical study of thermal fracture of ceramics materials in the water quench test. *J. Am. Ceram. Soc.*, 1987, **70**, 406–412.
4. Ishitsuka, M., Dato, T., Endo, T. and Shimada, M., Thermal shock fracture behaviour of ZrO_2 based ceramics. *J. Mat. Sci. Letters*, 1989, **24**, 4057–4061.
5. Baudín, C., Resistencia al choque térmico de materiales frágiles. *Anales de Mecánica de la Fractura*, 1990, **7**, 94–99.
6. Oguma, M. and Tanabe, I., Non-destructive evaluation of crack extension in UO_2 pellets subjected to thermal shock at various temperature differences. *Br. Ceram. Trans. J.*, 1990, **89**, 167–170.
7. Schneider, G. A., Thermal shock criteria for ceramics. *Ceram. Inter.*, 1991, **17**, 325–333.
8. Becher, P. F., Lewis III, D., Carman, K. R. and Gonzalez, A. C., Thermal shock resistance of ceramics: size and geometry effects in quench tests. *Ceram. Bull.*, 1980, **59**, 542–545.
9. Becher, P., Effect of water bath temperature on the thermal shock of Al_2O_3. *J. Am. Ceram. Soc.*, 1981, **1**, C17.
10. Singh, J. P., Tree, Y. and Hasselman, D. P. H., Effect of bath and specimen temperature on the thermal stress resistance of brittle ceramics subjected to thermal quenching. *J. Mat. Sci.*, 1981, **16**, 2109–2118.
11. Faber, K. T., Huang, M. D. and Evans, A. G., Quantitative studies of thermal shock in ceramics based on a novel technique. *J. Am. Ceram. Soc.*, 1981, **64**, 296–301.
12. Niihara, K., Singh, J. P. and Hasselman, D. P. H., Observations on the characteristics of a fluidized bed for thermal shock testing of brittle ceramics. *J. Mat. Sci.*, 1982, **17**, 2553–2559.
13. Marshall, D. B., Drory, M. D., Loh, R. L. and Evans, A. G., The thermal fracture of alumina. In *Fracture in ceramics materials*, ed. A. G. Evans. Noyes Publications, New Jersey, 1984, pp. 336–363.
14. Johnson-Walls, D., Drory, M. D. and Evans, A. G., Evaluation of reliability of brittle components by thermal stress testing. *J. Am. Ceram. Soc.*, 1985, **68**, 363–367.
15. Brockenbrough, J. R., Edgar Forsythe, L. and Rolf, R. L., Reliability of brittle materials in thermal shock. *J. Am. Ceram. Soc.*, 1986, **69**, 634–637.
16. Wei, G. C. and Walsh, J., Hot-gas-jet method and apparatus for thermal-shock testing. *J. Am. Ceram. Soc.*, 1989, **72**, 1286–1289.
17. Schneider, G. A. and Petzow, G., Thermal shock testing of ceramics — a new testing method. *J. Am. Ceram. Soc.*, 1991, **74**, 98–102.
18. Rogers, W. P. and Emery, A. F., Contact thermal shock of ceramics. *J. Mat. Sci.*, 1992, **27**, 146–152.
19. Awaji, H., Oguwa, M. and Sato, S., Testing method for thermal shock fracture of ceramics. In *Third Euro-Ceramics V. 3*, ed. P. Durán and J. F. Fernández. Faenza Editrice Iberica, S.L, Spain, 1993, pp. 883–888.
20. Olagnon, C., Fantozzi, G., Sudreau, F. and Peogne, P., Thermal shock and fatigue of mullite and alumina: refined analyses. In *Thermal Shock and Thermal Fatigue Behaviour of Advanced Ceramics*, ed. G. A. Schneider and G. Petzow, 1993, pp. 371–381.
21. Tomba, A. G., Choque térmico de alúmina densa. Ph.D. thesis, Universidad Nacional de Mar del Plata, Mar del Plata, 1998.
22. Gitzen, W. H., *Alumina as Ceramic Material*. The American Ceramic Society, Columbus, 1970.
23. Kingery, W. D., Factors affecting thermal stress resistance of ceramic materials. *J. Am. Ceram. Soc.*, 1955, **38**, 3–15.
24. Boley, B. A. and Weiner, J. H., *Theory of thermal stresses*. John Wiley & Sons, Inc, New York, 1985.
25. Munro, R. G., Evaluated material properties for a sintered α-alumina. *J. Am. Ceram. Soc.*, 1997, **80**, 1919–1928.